Mammalian Protein Expression Noise: Scaling Principles and the Implications for Knockdown Experiments

Marc R. Birtwistle[*,†,‡], Alexander von Kriegsheim[†], Maciej Dobrzyński[†], Boris N. Kholodenko[†], and Walter Kolch[†]

[*]Mount Sinai School of Medicine, Dept. Of Pharmacology and Systems Therapeutics, One Gustave L. Levy Place, Box 1215, New York, NY 10029
[†]Systems Biology Ireland, Conway Institute, University College Dublin, Belfield, Dublin 4, Republic of Ireland

[‡]To whom all correspondence should be addressed: Marc Birtwistle; P:++1-706-825-2803; F:++1-706-541-3951; E-mail: marc.birtwistle@gmail.com

Short Title: Mammalian Protein Expression Noise Scaling

Keywords: cell-to-cell variability, knock-down experiments, protein expression noise, bursting, probabilistic modeling

[§]**Abbreviations:**
cdf-cumulative density function; CV-Coefficient of Variation; DD-Degradation Domain; ERK-Extracellular Signal-Reguated Kinase; GAPDH-Glyceraldehyde 3-phosphate dehydrogenase; MEF-Mouse Embryonic Fibroblast; NF-κB-Nuclear Factor Kappa B; pdf-probability density function; PTEN-Phosphatase and tensin homolog; RKIP-Raf Kinase Inhibitor Protein; SEM-Standard Error of the Mean; SSE-Sum of Squared Errors; STAT3-Signal transducer and activator of transcription 3; YFP-Yellow Fluorescent Protein

Abstract

The abundance of a particular protein varies both over time within a single mammalian cell and between cells of a genetically identical population. Here, we investigate the properties of such noisy protein expression in mammalian cells by combining theoretical and experimental approaches. The gamma distribution model is well-known to describe cell-to-cell variability in protein expression in a variety of common scenarios. This model predicts, and experiments show, that when protein levels are manipulated by altering transcription rates or mRNA half-life, protein expression noise, defined as the squared coefficient of variation, is constant. In contrast, we also demonstrate that when protein levels are manipulated by changing protein half-life, as mean levels increase, noise decreases. Thus, in mammalian cells, the scaling relationship between mean protein levels and expression noise depends on how mean levels are perturbed. Therefore it may be important to consider how common experimental manipulations of protein expression affect not only mean levels, but also noise levels. In the context of knockdown experiments, natural cell-to-cell variability in protein expression implies that a particular cell from the knockdown population may have higher protein levels than a cell from the control population. Simulations and experimental data suggest that approximately three-fold knockdown in mean expression levels can reduce such so-called "overlap probability" to less than ~10%. This has implications for the interpretation of knockdown experiments when the readout is a single cell measure.

Introduction

Why do genetically identical cells exposed to the same conditions behave differently? One major reason seems to be that gene transcription and translation are inherently noisy processes; this has been reasonably well-studied in bacteria [1, 2] and yeast [3, 4], but to a lesser extent in mammalian systems [5, 6]. Most obviously, this noise can be viewed as problematic and something that cells must deal with, leading to the reinforced presence of network structures such as negative feedback and feedforward loop motifs that provide robustness to variability [7, 8]. Such non-genetic variability can also drive differential sensitivity to cancer drugs [9] and divergent cell-fate decisions [10]. However, while in some situations noise can hamper biological function, in others it may enhance it, by increasing signal sensitivity through stochastic focusing [11] or allowing a single cell type to take on a host of phenotypic abilities [12].

Gene expression noise can be classified as extrinsic or intrinsic. Extrinsic noise arises from fluctuations in the levels of entities facilitating gene expression such as, RNA polymerases, ribosomes, and translation and transcription factors, while intrinsic noise arises from factors internal to expression of the gene itself, such as low gene copy number [13, 14]. It has been shown in *E. coli* [15] and thought for other systems that for highly expressed genes, extrinsic noise dominates, while for most other genes intrinsic noise is more important. Primary influences on intrinsic noise are (i) the rate of transcription, which is burst-like due to the low number of genes for a particular protein in a cell [5, 16], and (ii) the number of proteins produced per mRNA, which is random probably due to competition between ribosomes and RNase for the mRNA [1, 2, 17]. Protein degradation also contributes to intrinsic noise, but in many cases to a much lesser extent than the aforementioned factors, since protein copy numbers are typically large enough to dampen the small stochastic fluctuations in degradation rate.

Given the significance of gene expression noise in mammalian systems, we asked two main questions to better understand it. First, do the molecular mechanisms by which mean protein expression levels are controlled in mammalian systems, such as transcription and protein degradation, have different control of noise? Second, how much must mean protein levels change such that a perturbed cell population has expression levels that are outside of the natural range of variability? This last question has implications for knockdown experiments, where the levels of a protein-of-interest are decreased (usually by RNAi), and then some biological response is observed in control and perturbed populations. In what follows, we combine theoretical modeling with experimental data to provide answers to these questions.

Results and Discussion

Relationships between cell-to-cell protein level distribution parameters and gene expression mechanisms

It has been well-established by both theory[5, 11, 18, 19] and experiments[15, 19-21] that in many situations, including those common in mammalian cells, cell-to-cell variability in protein expression levels is well-described by a gamma distribution. The gamma distribution is given by

$$N_{obs} \sim Gam(k_{obs}, \theta_{obs}); \; f(N_{obs}) = \frac{N_{obs}^{(k_{obs}-1)} e^{-N_{obs}/\theta_{obs}}}{(\theta_{obs})^{k_{obs}} \Gamma(k_{obs})} \qquad (1)$$

Here, N_{obs} is the experimentally observed protein expression level in a particular cell, f denotes the probability distribution function (pdf) of N_{obs}, and k_{obs} and θ_{obs} are the two parameters characterizing the experimentally observed distribution. Experimental data for the distributions of several proteins we commonly study are also well-described by Eq. 1 (Fig. 1A-D).

There are multiple mechanisms by which protein expression can be manipulated, which include altering: (i) chromatin organization dynamics; (ii) transcription rate; (iii) mRNA half-life; (iv) translation rate; and (v) protein half-life. However, the gamma distribution, which seems to provide a good description of protein expression variability, only contains two parameters, k_{obs} and θ_{obs}. Thus, these multiple biochemical mechanisms for changing protein expression levels must have at least some overlapping effects on protein expression noise, in terms of the parameters of the gamma distribution. Despite this inevitable overlap, however, it is possible that some of these biochemical mechanisms have unique effects on the gamma distribution parameters, and thus unique effects on protein expression noise.

Previous theoretical work has given insight into how gamma distribution parameters depend on biochemical mechanisms. When the lifetime of an mRNA is short relative to that of its corresponding protein (which is a frequent scenario in mammalian systems[22]), proteins are likely to be produced in bursts[18, 19]. Then, the gamma distribution parameter θ_{obs} corresponds to the burst size, or amount of protein produced per expression burst[18, 19]. Biochemically, one expects burst size to be affected significantly by transcription rate, mRNA half-life and translation rate. The former two affect the number of short-lived mRNAs being translated into protein during a burst, whereas the latter affects the number of proteins produced per mRNA. In fact, a major factor in control of protein levels in mammalian cells is translation rate[22]. The parameter k_{obs} is related to burst timing, i.e., to the number of past bursts that "persist" in the cell at any given time[18, 19]. By "persist", we mean that at least one of the proteins produced as a result of a particular burst is still within the cell and non-degraded. Biochemically, one might expect burst timing to be affected significantly by chromatin organization dynamics, since quicker chromatin opening events would lead to more frequent bursts[5], and protein half-life, since the quicker a protein is degraded, the fewer the number of past bursts that persist in the cell at any given time. Thus, it would seem that there is the potential for some level of independent control of gamma distribution parameters via biochemical mechanisms. In what follows we use this information to test scaling predictions of the gamma distribution model.

Scaling predictions of the gamma distribution model

One consequence of the gamma distribution is that the mean protein abundance (μ) should be linearly proportional to the standard deviation (σ), as long as k_{obs} is a constant (Fig. 2A)

$$\mu = k_{obs}\theta_{obs};\ \sigma^2 = k_{obs}(\theta_{obs})^2;\Rightarrow \sigma = \left(\frac{1}{\sqrt{k_{obs}}}\right)\mu \qquad (2)$$

Under these same conditions, protein expression noise, commonly defined as the squared coefficient of variation, should also be constant (Fig. 2B)

$$\eta = \frac{\sigma^2}{\mu^2} = \frac{1}{k_{obs}} \qquad (3)$$

Moreover, comparison of Eq. 2 and 3 shows that the slope of the linear dependency between μ and σ should be equal to the coefficient of variation (CV; CV=$\sqrt{\eta}$) (Fig. 2A-B).

To test these predictions experimentally, we would need to alter θ_{obs} without changing k_{obs}. Based on the considerations discussed above, k_{obs} should be predominantly related to burst timing, whereas θ_{obs} should be predominantly related to burst size. We reasoned that mRNA stability would preferentially alter burst size, since it would control the number of proteins produced from a particular mRNA. Thus, to test these scaling predictions we first used LS174 colon carcinoma cells where the levels of Raf Kinase Inhibitor Protein (RKIP) can be conditionally regulated using tetracycline (tet) or doxycycline (dox) inducible, shRNA mediated downregulation of RKIP[23]. We indeed saw excellent linear correlation between RKIP standard deviation and mean, and moreover, the CV was constant and approximately equal to the slope of the relationship between the standard deviation and mean (Fig. 2C-D).

It was previously shown that the effect of doxycycline on tet repressor-based expression plasmids is to affect transcription rates (burst sizes) but not burst frequencies[5]. We therefore thought that tet-regulated expression systems (for production of mRNA and protein as opposed to that for shRNA used above) should also follow Eqs. 2 and 3. We tested this prediction using two different engineered murine embryonic fibroblasts (MEFs) cell lines, where all three Ras genes had been knocked out, and then reconstituted with a tet-repressible wild type or V12 mutant K-Ras expression vector[24] . Both of these systems also obeyed the predicted scaling behavior, and the measured CV's were essentially constant and approximately equal to the slope derived from plotting mean vs. standard deviation (Fig. 2E-H). The fact that the same antibody was used to detect the wild type and mutant K-Ras proteins in different cell lines, yet they showed significantly different CVs, argues strongly that the observed noise is to a large extent attributable to biological mechanisms and not experimental artifacts. Thus, we propose that when transcription rates and mRNA half-lives are manipulated, mean protein levels are linearly proportional to the standard deviation, and this proportionality constant is the CV. Consistent with our results in mammalian cells, such scaling behavior between mean protein levels and the standard deviation was also reported for α-factor induced reporter YFP expression in *S. cerevisiae* [3]. Importantly, however, although these results are consistent with the predictions of a gamma distribution model, it remains unclear whether the fluctuations driving this noise are truly intrinsic, or are simply representing the upper extrinsic noise limit [15]. Indeed, it may be much more difficult than previously thought to clearly separate intrinsic and extrinsic noise contributions [25], and in fact some noise may be due to stochastic cell division [26], although in our experiments cells were serum-starved so such contribution should be minimal in this context. Nevertheless, more experiments will be needed to confirm what sources of fluctuations are driving the noise, and moreover, how general these scaling properties are in mammalian systems.

Our results up to this point suggest that protein expression noise is well-characterized by the gamma distribution, and that the gamma distribution parameters have biochemical meaning when such noise is introduced primarily by intrinsic factors. However, others have suggested that the lognormal and Weibull distributions also fit cell-to-cell protein expression variability well [10, 27]. The pdfs for a lognormal and Weibull random variable are, respectively,

$$f_{LN}(x) = \frac{1}{x\sqrt{2\pi\sigma_{LN}{}^2}} e^{-\left(\frac{(\ln x - \mu_{LN})^2}{2\sigma_{LN}{}^2}\right)} \quad \text{, and} \tag{4}$$

$$f_W(x) = \frac{k_W}{\lambda_W}\left(\frac{x}{\lambda_W}\right)^{(k_W-1)} e^{-\left(\frac{x}{\lambda_W}\right)^{k_W}} \quad . \tag{5}$$

Here, μ_{LN} and λ_W are the so-called scale parameters, which are analogous to the gamma distribution parameter θ_{obs}, whereas σ_{LN} and k_W are the so-called shape parameters, which are analogous to the gamma distribution parameter k_{obs}. If one varies the scale parameters of these distributions while holding the shape parameter constant, then the scaling behaviors of all three distributions are indistinguishable (Figs. 3A-D). The gamma distribution has a behavior that is distinct from the lognormal and Weibull distributions if one considers how protein expression noise scales with the mean protein expression if the scale parameter θ_{obs} is constant and the shape parameter k_{obs} is varied (Figs. 3E-G)

$$\eta = \frac{\sigma^2}{\mu^2} = \frac{k_{obs}\theta_{obs}{}^2}{\mu k_{obs}\theta_{obs}} = \frac{\theta_{obs}}{\mu}. \tag{6}$$

Specifically, for the gamma distribution, if θ_{obs} is constant, then protein expression noise should be inversely proportional to the mean protein expression, similar to what has been shown in previous theoretical work [28-30]. The above considerations suggested that k_{obs} can be altered by changing protein half-life [18, 19]. We therefore set out to test this prediction experimentally by using flow cytometry and a HEK293 cell line that contains a single copy of YFP tagged with a destabilizing domain (DD) domain. This system allows one to tune YFP half-life using an exogenous, cell-permeable ligand called Shield1, which binds to the DD domain and protects the protein from degradation [31]. Experimentally, we would expect that at low YFP expression levels, the observed CV^2 (η) would be equal to some upper limit corresponding to that of background autofluorescence and/or shot noise, and that at high expression levels, the observed η would correspond to some lower limit corresponding to that of the measurement technology, but between these limits we would see the scaling predicted by Eq. 6. We indeed confirmed that there is such a relationship between the squared coefficient of variation and mean protein expression levels (Fig. 3H). It is important to note that the large predicted increase in protein expression noise at low expression levels occurs at copy numbers of ~5-10 proteins/cell (Fig. 3G). Thus, with such flow cytometry experiments it is natural to expect that cellular autofluorescence will dominate the measured noise at these low expression levels, thus leading to the experimentally observed flat behavior at low mean levels rather than the theoretically predicted large increase. Moreover, these results do not prove that the log-normal and Weibull distributions are incorrect per se; their scale and shape parameters simply have no clear physical counterparts in a bursting gene expression model. It is in principle possible that some combination of parameter changes for the Weibull and log-normal distributions can yield similar scaling relationships.

Interestingly, this scaling behavior predicted by Eq. 6 was also reported for 43 proteins under 11 different environmental conditions in *S. cerevisiae*[4]. The fact that so

many different proteins would obey this simple scaling relationship with the same θ_{obs} parameter is somewhat surprising, and it implies that this parameter has a similar value for many different proteins in yeast. It is therefore tempting to speculate that in yeast, protein levels may be predominately regulated via control of protein stability and/or chromatin dynamics, as opposed to mRNA stability and transcription rate. This may explain why in general there seems to be much less correlation between protein and transcript levels than expected [15, 32]. However, this also depends on what mechanisms are controlling burst timing, which may well be due in part to translational bursting in mammalian cells [22, 33].

An evolutionary hypothesis follows from these scaling observations. Since noise seems to be differentially controlled by various protein expression mechanisms, and these mechanisms can be affected by genetic mutations, it follows that noise may be an evolvable trait that is subject to natural selection[33, 34]. In yeast, it was proposed that both essential genes and those involved in multi-unit complexes should evolve to have low expression noise; indeed, such genes were found to have a combination of high transcription rate with low translation rate that promotes low noise[34]. For multi-cellular organisms, however, the link between fitness and expression noise of individual genes is less clear. Until such knowledge is available, this point must remain an interesting speculation in mammalian systems. Nevertheless, it is interesting to note that functionally related proteins tend to have similar mRNA and protein half-life combinations [22], which seems to support the idea that expression noise is an evolvable trait in mammalian systems.

The impact of protein expression variability on knockdown experiments

Regardless of the distribution that cell-to-cell variability in protein expression follows, or even whether the system is at steady-state, the above analysis and a large body of previous work suggests protein expression variability can be quite large. This prompted us to consider noise in the context of a knockdown experiment, where one tries to decrease the mean protein expression levels, typically via RNA interference methods, and determine whether there is some biological effect of this knockdown. Given large amounts of expression noise, it is possible that a cell from the "knockdown" population may actually have higher expression levels than a cell from the "control" population. Thus, we were interested in how much "control" and "knockdown" cell populations overlap in a knockdown experiment, in terms of protein expression levels. This would be particularly relevant when the readout of such an experiment is a single cell measure. Analogous considerations may also be relevant for overexpression experiments, where the mean protein levels are increased rather than decreased. However, here we focus on knockdown experiments.

We mathematically define the overlap for a knockdown experiment as the probability that a cell from the knockdown population has higher protein levels than a cell in the control population, given a particular fold mean knockdown $f=\mu_p/\mu_c$, where μ_p and μ_c denote the mean protein levels in the perturbed and control populations (see Methods). For distributions similar to that shown in Fig. 1, this overlap can be significant for only two-fold mean knockdown (f=0.5; Fig. 4A-B). This is regardless of which gamma distribution parameters are changed to achieve knockdown (Fig. 4B). Greater than approximately three-fold mean knockdown is predicted to yield less than 10% overlap probability (Fig. 4B), which gives 90% confidence that a randomly chosen cell from the knockdown population has protein levels that are less than a randomly chosen cell from the control population.

To evaluate these predictions, we first used, as above, LS174 colon carcinoma cells where shRNA-mediated downregulation of RKIP can be controlled by dox (Fig. 4C-D). For this system, qualitative western blots suggested, and quantified flow cytometry data showed that the dox-induced downregulation of RKIP levels were at most two-fold. As predicted by theory, the RKIP distributions still displayed significant overlap. We therefore also tested the "Ras-less" MEFs as described above, where protein expression could be modulated over a wider dynamic range. In these "Ras-less" MEFs, treatment with dox for 24 hours results in an approximately two-fold knockdown, and control and knockdown populations substantially overlap. At 48 hours after dox treatment, however, the knockdown is approximately three-fold and the control and perturbed populations are almost completely separated (Fig. 4E-F). Transient transfection-based knockdown experiments of others [21](Fig. 4G-H) and our own (Fig. 4I) further support this hypothesis that less than three-fold knockdown is not sufficient to separate control and perturbed populations cleanly.

These results lead us to propose that less than three-fold knockdown can lead to substantial overlap between control and perturbed populations. We have, however, only tested a small subset of cases, and further experiments are required to determine how general this observation is. One potentially important consideration is transfection efficiency and potential variability in the resulting induction of the siRNA pathways. If a certain sub-population of cells did not initiate the RNAi pathway, we would expect bimodality in the observed protein expression distributions. In all of the cases we tested, which included both transient transfection and stable cell lines, this didn't seem to be an issue as observed by the unimodal, rather than bimodal, distribution of protein levels in the perturbed populations.

In terms of interpreting the results of a knockdown experiment, if one is interested in determining the population average effects of a particular knockdown, such as for example the mean levels of a downstream protein, then this overlap issue is likely not of immediate concern. This is because with enough sampling one can determine, to a desired level of confidence, whether a difference of means between the control and knockdown populations exists. Obviously, however, a greater difference of means gives a lower number of samples needed to observe effects. On the other hand, if one is using single-cell measurements as a readout for the effects of a knockdown experiment, then overlap may be a concern. Thus, in such cases when single-cell measurements are the readout of a knockdown experiment, we would propose a three-fold change heuristic for judging the efficacy of the knockdown.

Summary and Conclusions

We are starting to recognize that the variability in mammalian protein expression is large and can affect biological behavior. Therefore, we need tools to analyze it and to gauge its effects on outcomes in knockdown experiments. Such experiments are part of the standard repertoire of today's biology research and are facilitated by siRNA, microRNA and inducible expression technologies. One question is how much knockdown needs to be achieved to clearly link phenotypes to changes in protein expression. Based on our results, we suggest that knockdown of less than three-fold is within the physiological range of the variability of protein expression observed in individual cells. Thus, as a rule of thumb, any perturbation experiment involving changes in protein expression may be difficult to deconvolute in terms of *single cell responses* if the changes are less than threefold. On the other hand, mild (i.e. < threefold) knockdown might be practically used to study the *population average* effects of a protein knockdown in most cases. We also found that the

mechanism by which mean protein levels are changed can affect how protein expression noise scales with the mean. Our results suggest that, when proteins are produced in bursts (i.e. when protein half-life is much longer than mRNA half-life), changing mRNA half-life or transcription rates keeps noise constant, whereas increasing protein half-life decreases noise. Since it is becoming clearer that protein expression noise can play a major role in determining biological behavior, we should become aware of how our perturbations not only change mean protein expression levels, but also their noise levels, as such unrealized changes in noise may have confounding effects on the biological response.

Acknowledgements

We thank Alfonso Blanco in the Conway Institute Flow Cytometry Core Facility for his expertise and assistance with flow cytometry experiments, Oliver Rath for providing the inducible RKIP cell lines, Mariano Barbacid for providing the Ras-less MEFs, Christoph Waldner for providing YFP-DD HEK293s and the anonymous reviewers whose comments helped improve the manuscript.

Funding

This work was supported by Science Foundation Ireland [06/CE/B1129]. MRB acknowledges a Marie Curie International Incoming Fellowship [236758] and an EMBO long-term fellowship [ALTF 815-2010].

Materials and Methods

Definition of overlap probability in knockdown experiments. The probability that a cell from the control population has lower protein levels than a cell from the perturbed population in a knockdown experiment is related to the difference D between two independent gamma-distributed random variables,

$$D = N_c - N_p \ , \tag{7}$$

where N_c is the number of proteins in a randomly chosen cell of the control population and N_p is the number of proteins in a randomly chosen cell of the perturbed population. Let the mean fold change be μ_p/μ_c, where μ_c is the mean protein level in the control population and μ_p is the mean protein level in the perturbed population. The "overlap probability" is defined as the probability that a random variable D is smaller than zero for mean fold changes less than 1, which corresponds to artifacts in knockdown experiments. Thus, to investigate the overlap probability, we must analyze the pdf of D, f_D. In what follows we show how f_D can be cast in terms of a cross-correlation function.

Let $X_1 = N_c$ and $X_2 = -N_p$; X_1 and X_2 are independent random variables. The pdf of D, f_D, may be cast in terms of characteristic functions using the inversion formula[35]

$$f_D(d) = \frac{1}{2\pi}\int_{-\infty}^{\infty} e^{-itd}\varphi_1(t)\varphi_2(t)dt \ , \tag{8}$$

where φ_1 and φ_2 are respectively the characteristic functions of X_1 and X_2, i is the imaginary unit, and t is a dummy integration variable. The characteristic function of N_c is exactly that of X_1, whereas the characteristic function of N_p is the complex conjugate of the characteristic function for X_2,

$$\varphi_2 \equiv E[e^{iX_2 t}] = E[e^{-iN_p t}] = E[\cos(-N_p t) + i\sin(-N_p t)] = E[\cos(N_p t) - i\sin(N_p t)] = \overline{\varphi}_{N_p} \tag{9}$$

giving

$$f_D(d) = \frac{1}{2\pi}\int_{-\infty}^{\infty} e^{-itd}\varphi_{N_c}(t)\overline{\varphi}_{N_p}(t)dt \, , \tag{10}$$

Eq. 10 is equivalent to a Fourier transform of the product $\varphi_{N_c}(t)\overline{\varphi}_{N_p}(t)$ [35]. Denote the pdfs for N_c and N_p, respectively f_{Nc} and f_{Np}. From the definition of the cross-correlation function of f_{Np} and f_{Nc} , and from the cross-correlation theorem[36] we have,

$$f_{Np} \bigstar f_{Nc} \equiv \int_{-\infty}^{\infty} \overline{f}_{N_p}(\tau) f_{N_c}(d+\tau)\, d\tau = F\left[\overline{\varphi}_{N_p}(t)\varphi_{N_C}(t)\right], \qquad (11)$$

where τ is a dummy integration variable and F denotes a Fourier transform. It has been shown that Eq. 11 is equivalent to Eq. 10[36]. Thus, the pdf of D is given by the cross-correlation function of the pdfs of N_c and N_p (gamma densities with different parameters). We evaluate this cross-correlation function numerically with the MATLAB function *xcorr*.

Flow Cytometry for Intracellular Staining. Approximately $2x10^6$ adherent cells were lifted with trypsin, resuspended in growth medium containing full serum, centrifuged, and then resuspended in 1 mL of PBS. Then, 1 mL 6% formaldehyde in PBS was added and the solution incubated at 37°C for 10 minutes. The formaldehyde solution was removed by centrifugation, and then the cells were resuspended in ice-cold, 90% MeOH. At this point, cells are fixed and were stored for as long as one week before analysis. At the time of analysis, $5x10^5$ cells were taken and the MeOH solution removed by centrifugation. Cells were washed twice by centrifugation with Incubation Buffer (0.5 g BSA/100 mL PBS), resuspended in 90 μL of Incubation Buffer, and then the appropriate amount of primary antibody was added for 1 hour at room temperature. The cells were then washed twice by centrifugation in Incubation Buffer. If the primary antibody was not directly conjugated to a fluorophore, cells were resuspended in 90 μL of incubation buffer, and secondary antibody was added for 30 min to 1 hour at room temperature (two-fold the mass of primary antibody). Cells were then washed twice by centrifugation with Incubation Buffer, resuspended in 0.5 mL PBS, and analyzed on a flow cytometer. For all experiments, equal masses of a non-specific control antibody were used in parallel samples to verify that the signal of interest was specific to the antibody epitope. Moreover, for each primary antibody, dilutions were done to maximize the ratio of mean signal to the non-specific signal. Measurements were done using either a Cyan ADP flow cytometer with a 488 laser and 530/40 emission filter or an Accuri C6 with a 488 laser and 530/30 emission filter. Approximately 10,000 raw events were collected for each histogram, and these events were gated by forward and side scatter to eliminate debris, and by forward scatter height vs. area to eliminate doublets.

Flow Cytometry for YFP Expression. All buffers were supplemented with Shield1 (Clontech) concentrations matching the samples. Cells were washed with PBS and lifted with trypsin. Trypsin was inhibited by adding Soybean Trypsin Inhibitor and the cells were fixed in 1% paraformaldehyde for 15 minutes, centrifuged and resuspended in PBS. Measurements were done on an Accuri C6 with a 488 laser and 530/30 emission filter. Approximately 10,000 raw events were collected for each histogram, and these events were gated by forward and side scatter to eliminate debris, and by forward scatter height vs. area to eliminate doublets.as described above.

Cell Culture. A2780 cells were obtained from Jim Norman and grown in RPMI/10% FBS. LS174 cells and the RKIP shRNA variants were obtained and constructed as described previously [23], and were kept in RPMI/5% tet-free FBS (PAA, Pennsylvania, USA). Ras-less MEFs with inducible, tet-off K-Ras repression were obtained from Mariano Barbacid [24], and kept in DMEM/10% FBS with G418 (Sigma). All growth media was supplemented with standard concentrations of penicillin/streptomycin and L-Glutamine. For experiments with inducible LS174 cells, doxycycline (Sigma) was added to the growth media in the indicated concentrations for 48 hours. For experiments with inducible Ras-less MEFs, doxycycline was either added to the growth media at 100 ng/mL for the indicated times, or added for 48 hrs at the indicated concentrations. Both the LS174 and Ras-less MEFs were serum starved for 16 hours prior to harvesting. The DD-YFP expressing HEK-293 (clone 19-3-1) cells were obtained from Christoph Waldner[31] and cultivated in DMEM with 10% FBS and 1 μg/ml puromycin. Cells were plated in a 12-well dish and, prior to FACS analysis, starved in serum-free DMEM for 20h. Simultaneously with starvation, YFP-DD was stabilized by adding Shield1 (Clontech) at concentrations of 0, 0.00625, 0.0125, 0.025, 0.04, 0.05, 0.2, 0.5, 1, 2, and 4 μM (all in at least triplicate).

Western Blotting. LS174 cell populations were treated as indicated, then lysed and subjected to western blot analysis as previously described[23].

Antibodies. For flow cytometry, the following antibodies were used: rabbit polyclonal 07-137 for RKIP (Millipore), rabbit monoclonal 5084 Alexa 488 conjugate for Akt (Cell Signaling), rabbit monoclonal 3906 Alexa 488 conjugate for GAPDH (Cell Signaling), mouse monoclonal OP40 Anti-pan-ras for K-Ras and K-RasV12 (Calbiochem), Goat F(ab')2 fragments of anti-rabbit or anti-mouse Alexa 488 conjugate for secondaries (Invitrogen), mouse monoclonal 4878 or rabbit monoclonal 2975 Alexa 488 conjugates for non-specific controls in experiments with fluorescent primary antibodies (Cell Signaling), and mouse monoclonal 4097 or rabbit monoclonal 3900 for non-specific controls in experiments with fluorescent secondary antibodies (Cell Signaling). For western blotting, we used rabbit polyclonal 07-137 for RKIP (Millipore) and rabbit polyclonal M5670 for ERK (Sigma).

siRNA Knockdown of GAPDH. Approximately 10^6 exponentially growing A2780 cells were harvested and then resuspended in Amaxa nucleofector solution T (Lonza) containing 5 μL of a 20 pmol/uL solution of a GAPDH or non-targeting pool of 4 siRNAs (Fisher; Dharmacon ON-TARGETplus Human SMARTpools). The cells were then transfected with the siRNA pool via electroporation with the Amaxa nucleofector (Lonza) using program T-024. After transfection, cells were plated and grown in full growth medium. After 48 hours, the cells were subjected to flow cytometry analysis as described above.

References

1. L. Cai, N. Friedman and X. S. Xie, *Nature*, 2006, **440**, 358-362.
2. J. Yu, J. Xiao, X. Ren, K. Lao and X. S. Xie, *Science*, 2006, **311**, 1600-1603.
3. A. Colman-Lerner, A. Gordon, E. Serra, T. Chin, O. Resnekov, D. Endy, C. G. Pesce and R. Brent, *Nature*, 2005, **437**, 699-706.
4. A. Bar-Even, J. Paulsson, N. Maheshri, M. Carmi, E. O'Shea, Y. Pilpel and N. Barkai, *Nat Genet*, 2006, **38**, 636-643.
5. A. Raj, C. S. Peskin, D. Tranchina, D. Y. Vargas and S. Tyagi, *PLoS Biol*, 2006, **4**, e309.
6. A. Sigal, R. Milo, A. Cohen, N. Geva-Zatorsky, Y. Klein, Y. Liron, N. Rosenfeld, T. Danon, N. Perzov and U. Alon, *Nature*, 2006, **444**, 643-646.
7. W. Ma, A. Trusina, H. El-Samad, W. A. Lim and C. Tang, *Cell*, 2009, **138**, 760-773.
8. T. Nakakuki, M. R. Birtwistle, Y. Saeki, N. Yumoto, K. Ide, T. Nagashima, L. Brusch, B. A. Ogunnaike, M. Okada-Hatakeyama and B. N. Kholodenko, *Cell*, 2010, **141**, 884-896.
9. A. A. Cohen, N. Geva-Zatorsky, E. Eden, M. Frenkel-Morgenstern, I. Issaeva, A. Sigal, R. Milo, C. Cohen-Saidon, Y. Liron, Z. Kam, L. Cohen, T. Danon, N. Perzov and U. Alon, *Science*, 2008, **322**, 1511-1516.
10. S. L. Spencer, S. Gaudet, J. G. Albeck, J. M. Burke and P. K. Sorger, *Nature*, 2009, **459**, 428-432.
11. J. Paulsson, O. G. Berg and M. Ehrenberg, *Proc Natl Acad Sci U S A*, 2000, **97**, 7148-7153.
12. M. Thattai and A. van Oudenaarden, *Genetics*, 2004, **167**, 523-530.
13. J. M. Raser and E. K. O'Shea, *Science*, 2005, **309**, 2010-2013.
14. P. S. Swain, M. B. Elowitz and E. D. Siggia, *Proc Natl Acad Sci U S A*, 2002, **99**, 12795-12800.
15. Y. Taniguchi, P. J. Choi, G. W. Li, H. Chen, M. Babu, J. Hearn, A. Emili and X. S. Xie, *Science*, 2010, **329**, 533-538.
16. J. M. Pedraza and J. Paulsson, *Science*, 2008, **319**, 339-343.
17. H. H. McAdams and A. Arkin, *Proc Natl Acad Sci U S A*, 1997, **94**, 814-819.
18. N. Friedman, L. Cai and X. S. Xie, *Phys Rev Lett*, 2006, **97**, 168302.
19. V. Shahrezaei and P. S. Swain, *Proc Natl Acad Sci U S A*, 2008, **105**, 17256-17261.
20. A. A. Cohen, T. Kalisky, A. Mayo, N. Geva-Zatorsky, T. Danon, I. Issaeva, R. B. Kopito, N. Perzov, R. Milo, A. Sigal and U. Alon, *PLoS One*, 2009, **4**, e4901.
21. P. LaPan, J. Zhang, J. Pan, A. Hill and S. A. Haney, *BMC Cell Biol*, 2008, **9**, 43.
22. B. Schwanhausser, D. Busse, N. Li, G. Dittmar, J. Schuchhardt, J. Wolf, W. Chen and M. Selbach, *Nature*, 2011, **473**, 337-342.
23. S. Y. Shin, O. Rath, S. M. Choo, F. Fee, B. McFerran, W. Kolch and K. H. Cho, *J Cell Sci*, 2009, **122**, 425-435.
24. M. Drosten, A. Dhawahir, E. Y. Sum, J. Urosevic, C. G. Lechuga, L. M. Esteban, E. Castellano, C. Guerra, E. Santos and M. Barbacid, *EMBO J*, 2010, **29**, 1091-1104.
25. A. Hilfinger and J. Paulsson, *Proc Natl Acad Sci U S A*, 2011, **108**, 12167-12172.

26. D. Huh and J. Paulsson, *Nat Genet*, 2011, **43**, 95-100.
27. J. Gunawardena, *Proceedings of the Ieee*, 2008, **96**, 1386-1397.
28. M. Thattai and A. van Oudenaarden, *Proc Natl Acad Sci U S A*, 2001, **98**, 8614-8619.
29. E. M. Ozbudak, M. Thattai, I. Kurtser, A. D. Grossman and A. van Oudenaarden, *Nat Genet*, 2002, **31**, 69-73.
30. J. Paulsson, *Nature*, 2004, **427**, 415-418.
31. C. Waldner, O. Rempel, F. Schutte, M. Yanik, N. Solomentsew and G. U. Ryffel, *BMC Res Notes*, 2011, **4**, 420.
32. S. Rogers, M. Girolami, W. Kolch, K. M. Waters, T. Liu, B. Thrall and H. S. Wiley, *Bioinformatics*, 2008, **24**, 2894-2900.
33. M. Kaern, T. C. Elston, W. J. Blake and J. J. Collins, *Nat Rev Genet*, 2005, **6**, 451-464.
34. H. B. Fraser, A. E. Hirsh, G. Giaever, J. Kumm and M. B. Eisen, *PLoS Biol*, 2004, **2**, e137.
35. B. A. Ogunnaike, *Random phenomena : fundamentals of probability and statistics for engineers*, CRC Press, Boca Raton, FL, 2010.
36. E. W. Weisstein, *"Cross-Correlation Theorem." From MathWorld--A Wolfram Web Resource*, http://mathworld.wolfram.com/Cross-CorrelationTheorem.html, Accessed 21 July, 2012.

Figure Legends

Figure 1. Fit of the Gamma Distribution to Various Experimental Data. Dotted lines correspond to data, whereas solid black lines correspond to gamma distribution fits. Gamma distribution parameter values were obtained by maximum likelihood estimation. Cells were serum-starved for at least 16 hours prior to the experiment. (**A**) RKIP abundance in a population of LS174 colon carcinoma cells (k_{obs}*=4.6;* θ_{obs}*=10,800 [AU]*). (**B**) GAPDH abundance in a population of A2780 ovarian carcinoma cells (k_{obs}*=7.58;* θ_{obs}*=2,000 [AU]*). (**C**) Akt abundance in a population of A2780 cells (k_{obs}*=8.15;* θ_{obs}*=13.5 [AU]*). (**D**) K-RasV12 abundance in a population of Ras-less MEF cells expressing doxycycline-downregulatable K-RasV12 (k_{obs}*=3.51;* θ_{obs}*=5.47x10^4 [AU]*).

Figure 2. Effects of mRNA Half-Life and Transcription Rates on Protein Expression Noise. (**A-B**) Scaling predictions between the mean (μ) and the standard deviation (σ) or the coefficient of variation (CV) in the scenario that k_{obs} is constant and θ_{obs} is changed to manipulate mean protein levels. (**C-D**) Dependence of the standard deviation and CV on mean RKIP levels in LS174 cells with tet-inducible shRNA against RKIP. Mean RKIP levels were altered using various doses of doxycycline semilogarithmically spanned between 5 and 0.1 ng/mL. (**E-F**) Dependence of the standard deviation and CV on mean wild type K-Ras levels in engineered MEFs. Mean K-Ras levels were altered using various doses of doxycycline. In E-H, dox concentrations were varied semilogarithmically between 1 and 0.01 ng/mL. (**G-H**) Dependence of the standard deviation and CV on mean K-Ras-V12 levels in engineered MEFs. Mean K-Ras-V12 levels were altered using various doses of doxycycline as indicated above.

Figure 3. Effects of Protein Half-Life on Protein Expression Noise. (**A-B**) Parametric plots of scaling relationships for the lognormal distribution where the shape parameter (σ_{LN}) is held constant at 0.1 and the scale parameter (μ_{LN}) is varied linearly between 0.1 and 8. (**C-D**) Scaling relationships for the Weibull distribution where the scale parameter (λ_W) is held constant at 0.5 and the shape parameter (k_W) is varied linearly between 1 and 100. (**E**) Scaling relationship for the lognormal distribution where the shape parameter (σ_{LN}) is varied linearly between 0.1 and 4 and the scale parameter (μ_{LN}) is held constant at 0.1. (**F**) Scaling relationships for the Weibull distribution where the scale parameter is varied linearly between 0.1 and 1 and the shape parameter is held constant at 0.001. (**G**) Scaling relationship for the gamma distribution where the shape parameter (k_{obs}) is varied between 1 and 100 and the scale parameter θ_{obs} is held constant at 10. (**H**) Relative mean YFP fluorescence plotted against protein expression noise in a population of isogenic HEK293 cells where YFP levels are altered by stabilizing the protein. Black squares correspond to flow cytometry data, whereas the black solid line corresponds to $\begin{cases} y = 0.037/x; x \geq 0.125 \\ y = 0.534; 0 \leq x < 0.125 \end{cases}$.

Figure 4. Effects of Noise on Knockdown Experiments. (**A**) The simulated effects of two- and five-fold mean knockdown (blue) on the protein expression distribution given the gamma distribution model with k_{obs}*=6*, which is typical based on the measurements in Fig. 1. Knockdown was simulated by changing the scale parameter θ_{obs} by the indicated fold change (from 50,000). The relationships between these

distributions were independent of the initial value of θ_{obs}. (**B**) Simulations of the overlap probability between control and perturbed cell populations as a function of mean fold expression change. The overlap probability quantifies the probability that a cell in the control population has lower expression than that of knockdown population (see Methods). The mean of the gamma distribution is equal to the product $k_{obs}\theta_{obs}$, and therefore can be changed by varying either k_{obs} or θ_{obs}. We simulated several possibilities within the range of observed k_{obs} values (between 4 and 8). All combinations show the same trend. Starting with different absolute values of θ_{obs} did not change these results. (**C**) Flow cytometery measurements of RKIP abundance in LS174 cells with tet-inducible shRNA against RKIP. Western blot data corresponding to these same conditions are shown above the flow cytometry data. Data are representative of three independent experiments. (**D**) Population means calculated from the flow cytometry data for the conditions shown in Panel C. Only approximately 1.5 to two-fold mean knockdown are observed at a maximum, which explains the large overlap between the distributions in Panel C. (**E**) Flow cytometry measurements of K-Ras abundance in MEFs where K-Ras expression is controlled with a tet-off promoter. (**F**) Population means calculated from the data in Panel E. Approximately three-fold knockdown after 48 hrs of dox treatement separates the control and perturbed populations cleanly. Where applicable, errors bars correspond to SEM from three independent experiments. (**G-H**) Data are from Lapan et al., 2008[21], Fig. 3A and Fig. 4A. In Panel G, PTEN was knocked down with siRNA in MDA-MB-231 cells, and in Panel H, STAT3 was knocked down with siRNA in SW480 cells. In both panels, abundance was assayed by immunofluorescence microscopy. (**I**) Effects of approximately 2-fold GAPDH knockdown in A2780 cells as measured by flow cytometry.

Figure 1, Birtwistle et al.

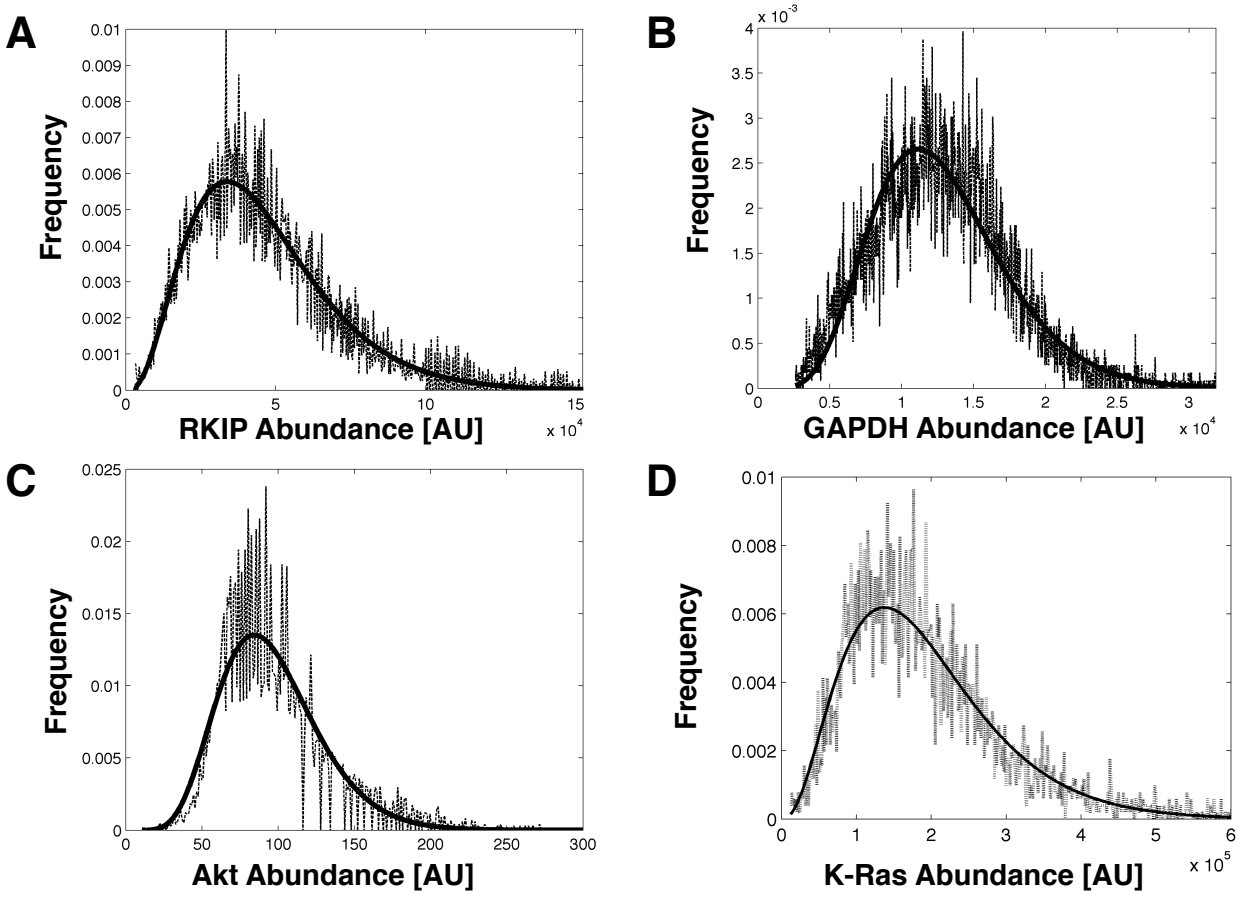

Figure 2, Birtwistle et al.

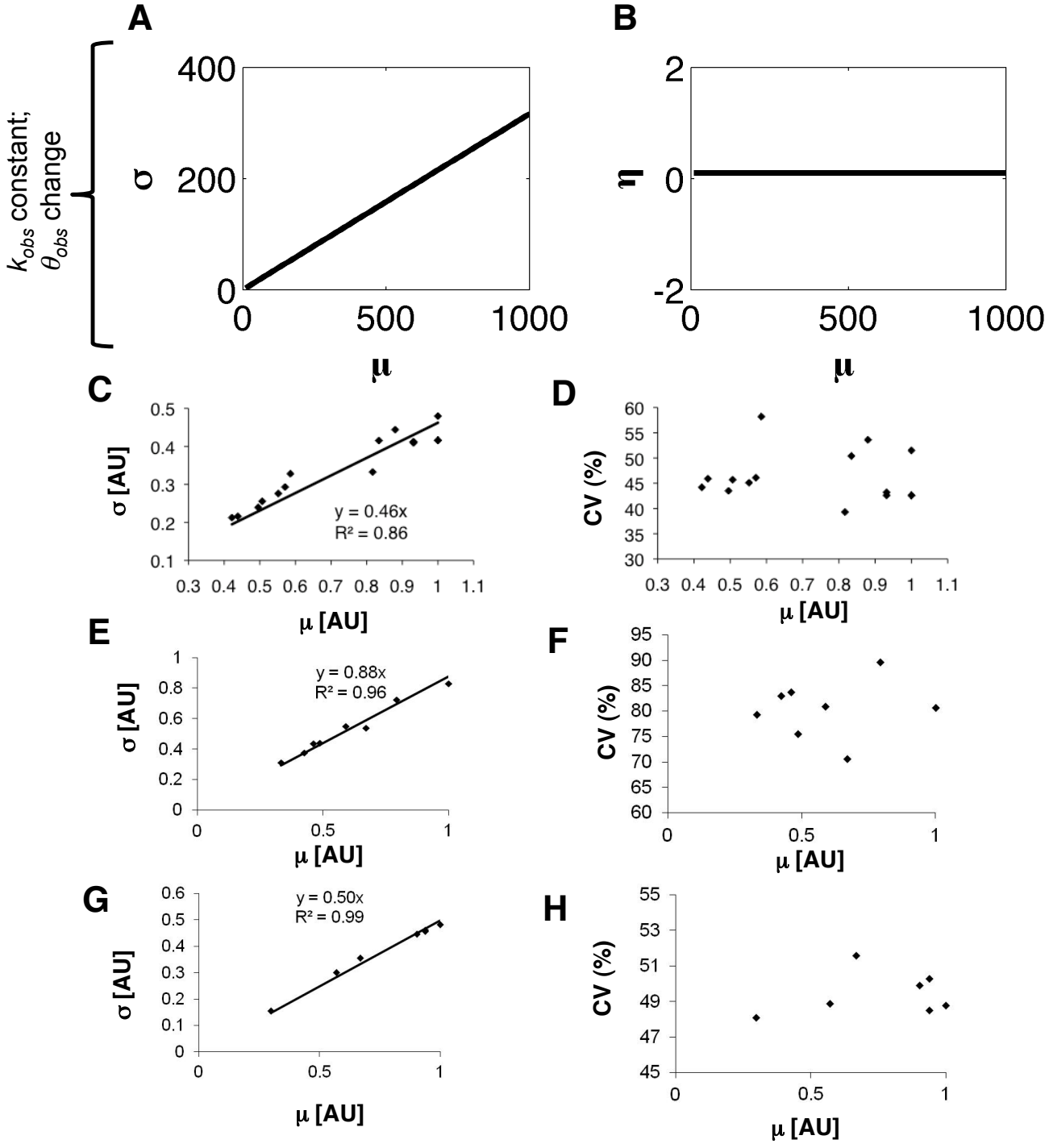

Figure 3, Birtwistle et al.

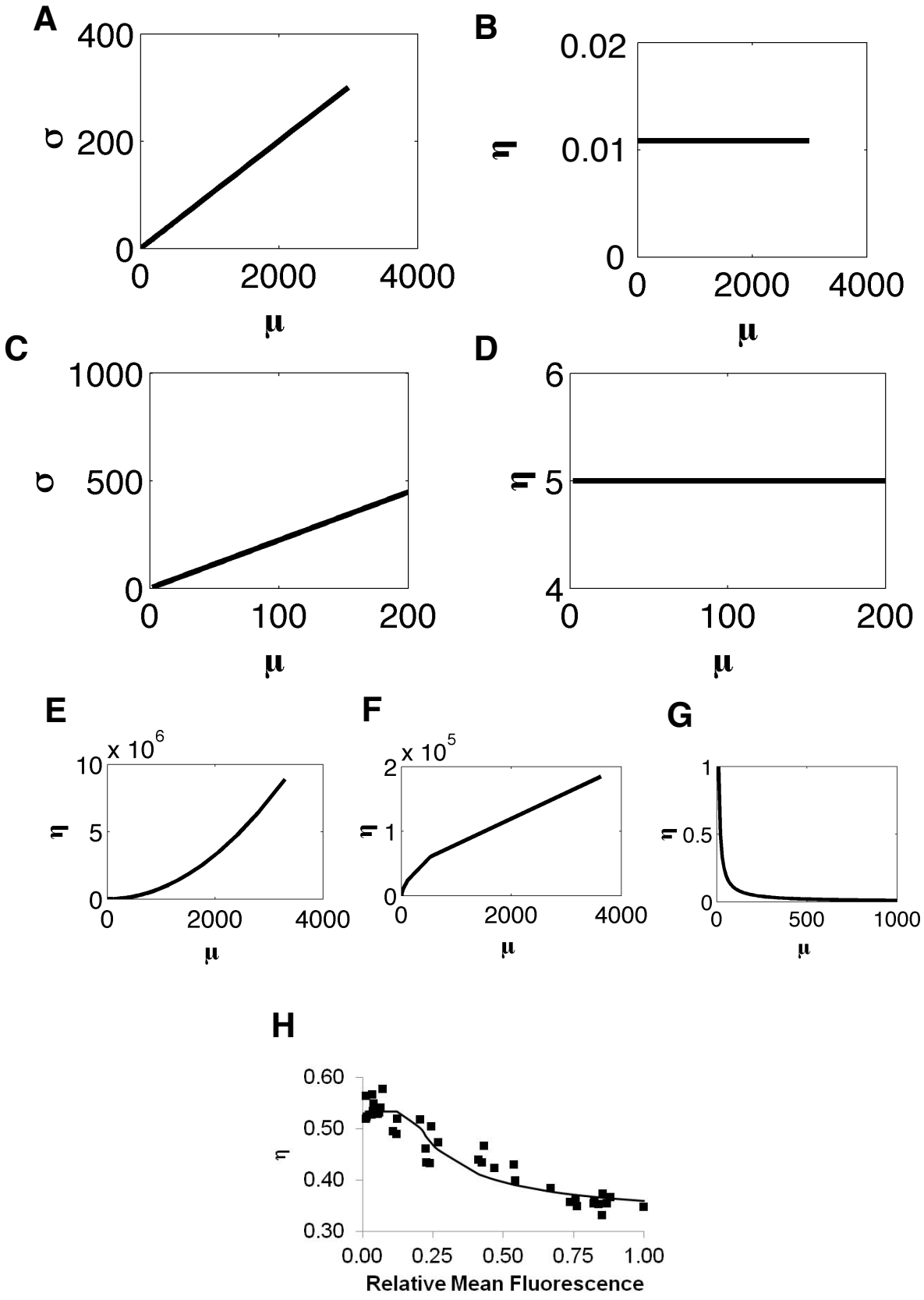

Figure 4, Birtwistle et al.